

Research Paper

Fabrication of Na-W Co-Doped Exfoliated G-C₃N₄ Nanoparticles for Methylene Blue Removal

Mohammad Javad Hakimi-Tehrani, Sayed Ali Hassanzadeh-Tabrizi*, Narjes Koupaei, Ali Saffar, Mahdi Rafiei

Advanced Materials Research Center, Department of Materials Engineering, Najafabad Branch, Islamic Azad University, Najafabad, Iran.

ARTICLE INFO

Article history:

Received 8 July 2022

Accepted 30 August 2022

Available online 1 September 2022

Keywords:

Nanomaterials

Carbon nitride

Doping

Photocatalyst

ABSTRACT

Bulk g-C₃N₄ has very poor photocatalytic activity. Many methods have been utilized to increase the photocatalytic performance of this semiconductor. Here, a simple preparation was used to create exfoliated g-C₃N₄ that was co-doped with sodium and tungsten. The produced Na-W co-doped exfoliated g-C₃N₄ was characterized using X-ray diffraction (XRD), transmission electron microscopy (TEM), UV-vis spectroscopy, and Fourier transform infrared spectroscopy (FTIR), X-ray photoelectron spectroscopy (XPS). The doping samples with Na and W changed the band structure of the g-C₃N₄ lattice, which increased light absorption and caused a reduction in the band gap. The samples had layered morphology. After exfoliation and sodium and tungsten co-doping of the samples, the methylene blue photodegradation was greatly enhanced. The doping of the samples also had an impact on the dye adsorption capacity. The dye removal activity of the Na-W co-doped exfoliated g-C₃N₄ sample is higher than those of pure bulk g-C₃N₄ and pure exfoliated g-C₃N₄. The rate reaction constant (k) of the Na-W co-doped exfoliated g-C₃N₄ is up to 3.3 times greater than that of bulk g-C₃N₄. The produced photocatalyst may be utilized for the treatment of wastewater comprising methylene blue as the pollutant agent.

Citation: Hakimi-Tehrani, M.J.; Hassanzadeh-Tabrizi, S.A.; Koupaei, N.; Saffar, A.; Rafiei, M. (2022). Fabrication of Na-W Co-Doped Exfoliated G-C₃N₄ Nanoparticles for Methylene Blue Removal, Journal of Advanced Materials and Processing, 10 (4), 3-11. Dor: 20.1001.1.2322388.2022.10.4.1.0

Copyrights:

Copyright for this article is retained by the author (s), with publication rights granted to Journal of Advanced Materials and Processing. This is an open – access article distributed under the terms of the Creative Commons Attribution License (<http://creativecommons.org/licenses/by/4.0>), which permits unrestricted use, distribution and reproduction in any medium, provided the original work is properly cited.



* **Corresponding Author:**

E-Mail: dralihassanzadeh@gmail.com

1. Introduction

Dealing with the problem of sustainable world development is becoming extremely difficult due to rising alarming environmental concerns and energy demand. Organic dyes are one of the important sources of pollution in the water [1]. These toxic materials could cause lots of problems for aquatic ecosystems. In addition, these materials cause some serious diseases in humans, like different kinds of cancer [2]. A promising method for removing such organic compounds from water while employing clean solar energy is to use photocatalysts, which are based on semiconductor materials. Many kinds of photocatalyst semiconductors have been used recently [3]. Among different semiconductors, g-C₃N₄ is a unique one due to its exceptional physical and chemical characteristics, such as heat tolerance, chemical resistance, low price and unique optical properties [4, 5]. This semiconductor is practically insoluble in water and many nonpolar solvents like toluene, ethanol, etc. In addition, it maintains its structure until 700 °C. The g-C₃N₄ has a band gap of about 2.7 eV to effectively absorb visible light [6]. However, the absorption range is limited, being less than 500 nm [7]. High electron-hole recombination is another barrier to the use of this semiconductor as an effective photocatalyst. As a result, ongoing attempts have been made to enhance its performance [8].

Different methods have been used, such as coupling with other semiconductors or doping with different elements [9, 10]. Heterogeneous nano-semiconductors used as photocatalysts improve the rate of reactions due to the increase in the surface-to-volume ratio [11]. As it is known, this phenomenon provides lots of active sites leading to better catalytic yield. The modification of the surface texture is also used to improve photocatalytic activities [12–15]. Doping of semiconductors with different kinds of metal ions is an effective strategy to improve their photoreactions. Various metal ions doping has been used so far to improve the photocatalytic properties of carbon nitride. For example, iron [16–18], nickel [19], sodium [20], and potassium [21] are some of the metal ions that have been used so far.

In this work, an exfoliated porous g-C₃N₄ was prepared by two-step heat treatment to control the surface of particles. Moreover, sodium and tungsten were co-doped with exfoliated g-C₃N₄ to improve the photocatalytic properties and reduce electron-hole recombination. The produced composite was characterized via different methods. In addition, the photocatalytic properties of the samples were studied via the photodegradation of methylene blue as a pollutant model.

2. Experimental procedure

Urea (CH₄ N₂ O, Sinchem) and sodium tungstate dihydrate (H₄Na₂O₆W, Sigma Aldrich) were utilized

for the fabrication of Na-W co-doped exfoliated g-C₃N₄ nanoparticles. In order to create exfoliated g-C₃N₄, a thermal heat treatment approach was used in the solid state. The urea undergoes breakdown during calcination. Because no additional chemicals were used during the heat treatment, it has the advantages of simplicity, affordability, and environmental friendliness. For this aim, 10 g urea was heated for two hours at 555 °C until it thermally broke down and produced g-C₃N₄. For the exfoliation of the powders, a secondary heat treatment was performed. For this aim, the produced powders were then ground and calcined for three hours at 355 °C. For the addition of Na-W to the samples, sodium tungstate dihydrate was mixed with urea. The next steps of the process were similar to the production of the exfoliated g-C₃N₄.

XRD patterns were obtained via a Philips PW3040 Diffractometer with a copper source. A TEM instrument (CM120 microscope) was used for the investigation of the morphology. A PerkinElmer PHI 5000 C ESCA instrument (Al K α) was used for X-ray photoelectron spectroscopy (XPS). UV-vis instrument (Shimadzu UV-2450 spectrophotometer) was used for the study of the optical properties of samples. Fourier transformed infrared (FTIR) spectra were obtained on an Avatar Thermo instrument.

For the investigation of the photocatalytic properties of the samples, 50 mg of the specimens were dispersed in 50 mL of methylene blue solution (10 ppm). The mixture was stirred in the dark for 30 min to create the adsorption-desorption equilibrium. Then the glass container was exposed to light for 90 min. After the illumination of light, the powder was removed from the solution by centrifugation. A 3220UV UV-visible spectrophotometer was used to investigate the absorbance of samples at 664 nm. The amounts of absorbance, with the aid of the calibration curve, gave the amount of pollutant in the solution.

3. Results and discussion

The XRD patterns of the synthesized g-C₃N₄ and Na-W co-doped g-C₃N₄ nanoparticles are displayed in Fig. 1. Two peaks at 13.1° and 27.3°, which correspond to the (100) and (002) crystal planes of g-C₃N₄ (JCPDS 87-1526), are visible in the patterns of the samples. The intensity of these two peaks reduces as Na-W elements are added to the samples. It indicates that graphitic carbon nitride crystal formation is hindered. It was reported that faster charge transfer and separation are facilitated by the smaller crystal size [22]. The Na-W co-doped g-C₃N₄ nanoparticles pattern shows no peak for the compounds related to the sodium and tungsten, which is due to low amounts of these elements in the samples. In addition, the doped sample shows a peak shift toward a lower 2 theta value. This was most likely caused by ions doping in graphitic carbon nitride sites, which may increase the interlayer gap.

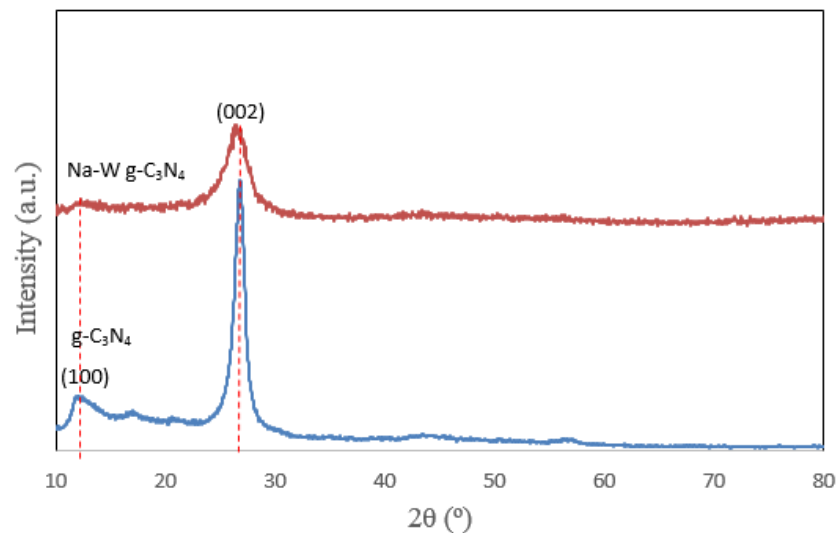


Fig. 1. XRD patterns of the g-C₃N₄ and Na-W co-doped g-C₃N₄.

By using FTIR spectroscopy, the chemical bonds of pure g-C₃N₄ and Na-W co-doped g-C₃N₄ are further investigated (Fig. 2). Since both of the samples have similar FTIR spectra, their fundamental chemical structures are the same. The vibration modes of the s-triazine ring and the stretching vibration modes of various C-N bonds are responsible for the peaks at

810 cm⁻¹ and 1200 to 1800 cm⁻¹, respectively [23, 24]. The vibration bonds of -OH and -NH₂ on the sample surface are responsible for the peak at around 3000-3500 cm⁻¹ [25]. The similarity of these patterns confirms that Na and W ions doping does not destroy the chemical structure of the graphitic carbon nitride.

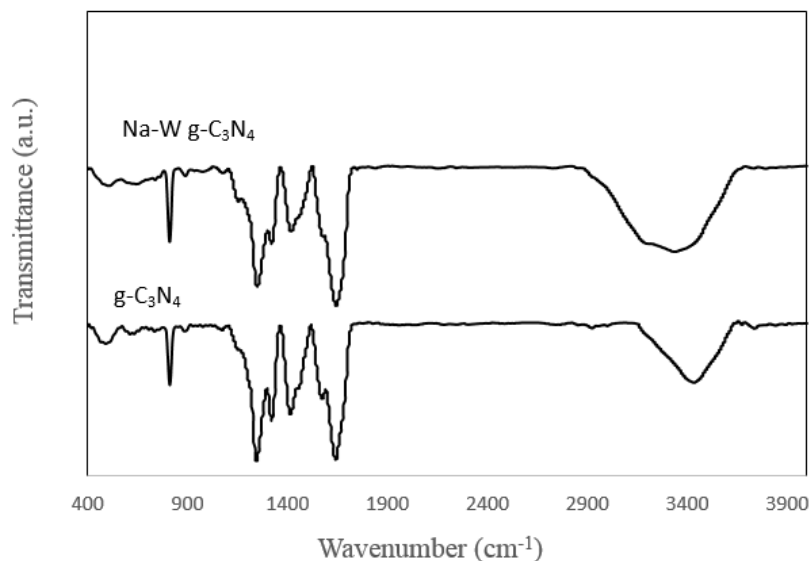


Fig. 2. FTIR spectra of the g-C₃N₄ and Na-W co-doped g-C₃N₄.

The optical absorption of Na-W co-doped g-C₃N₄ and pure g-C₃N₄ was studied using UV-vis diffuse reflectance spectra (Fig. 3). The square root of the Kubelka-Munk functions is plotted against the photon energy, and the tangent lines in those plots are used to estimate the band gaps (Fig. 4). The major absorption edge of g-C₃N₄ is around 460 nm. After doping, the absorption of light increases, which may improve the photocatalytic activity of doped samples. About 2.72 eV is the band gap for g-C₃N₄ and is in good agreement with the value reported in earlier literature [26, 27]. The apparent red changes of the

absorption band are shown in the Na-W co-doped g-C₃N₄ sample. As a result, the hue of the samples darkens as the Na and W ions increase. The band gap energy decreases from 2.72 to 2.64 eV after the addition of the elements. This suggests that the optical characteristics and band structure of the graphitic carbon nitride have a strong relationship with the doping process. Following Na and W ions doping, an orbital hybridization may occur, changing the potential of the valance band and conduction band [22].

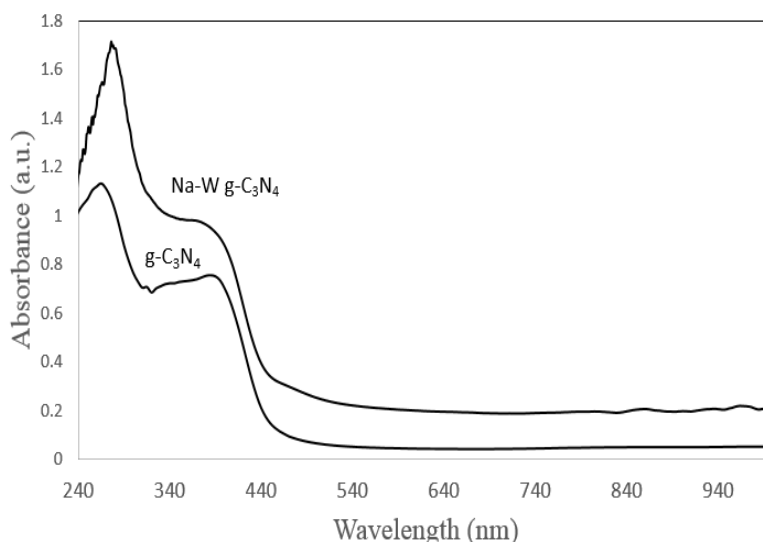


Fig. 3. Uv-vis spectra of the g-C₃N₄ and Na-W co-doped g-C₃N₄.

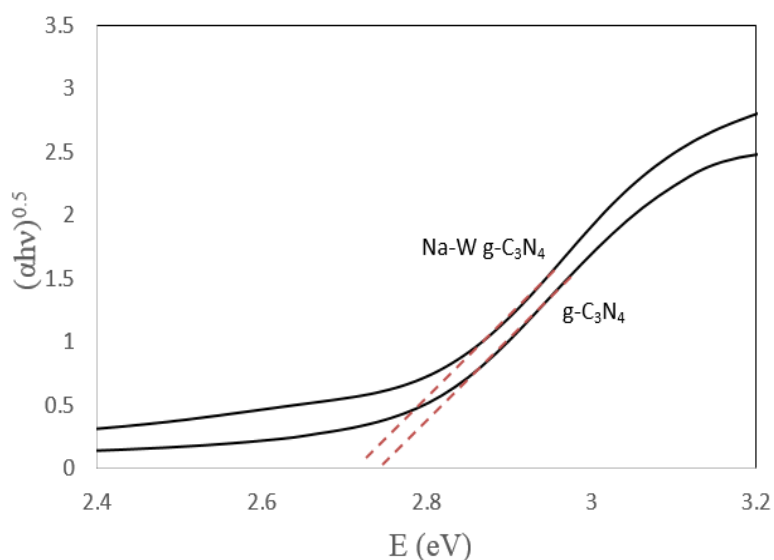


Fig. 4. Calculation of band gap energy of the g-C₃N₄ and Na-W co-doped g-C₃N₄.

Due to low amounts of doping elements, XRD results could not be shown the existence of sodium and tungsten. Therefore, XPS can be used to characterize chemical species that are present close to the catalyst surface. Fig. 5 displays the XPS spectra of the surface of samples in the energy regions of Na and W elements. As can be seen, both doped elements were detected on the surface of the samples. The peak with a binding energy of 1071 eV indicates the presence of sodium ions [28]. In addition, two peaks at 34.8

and 37.0 eV could be attributed to the W 4f_{7/2} and W 4f_{5/2}, respectively [29]. Since Na (about 0.1 nm) and W (about 0.6 nm) have far greater ionic radii than C (about 0.07 nm) and N (about 0.065 nm), therefore, substitutional doping shouldn't happen. Additionally, g-C₃N₄ is a covalent molecule. Na and K ions could not be doped in a substitutional site as an ion state. This demonstrates that there was no substitutional doping, and it is highly probable that only interstitial doping happened in the samples.

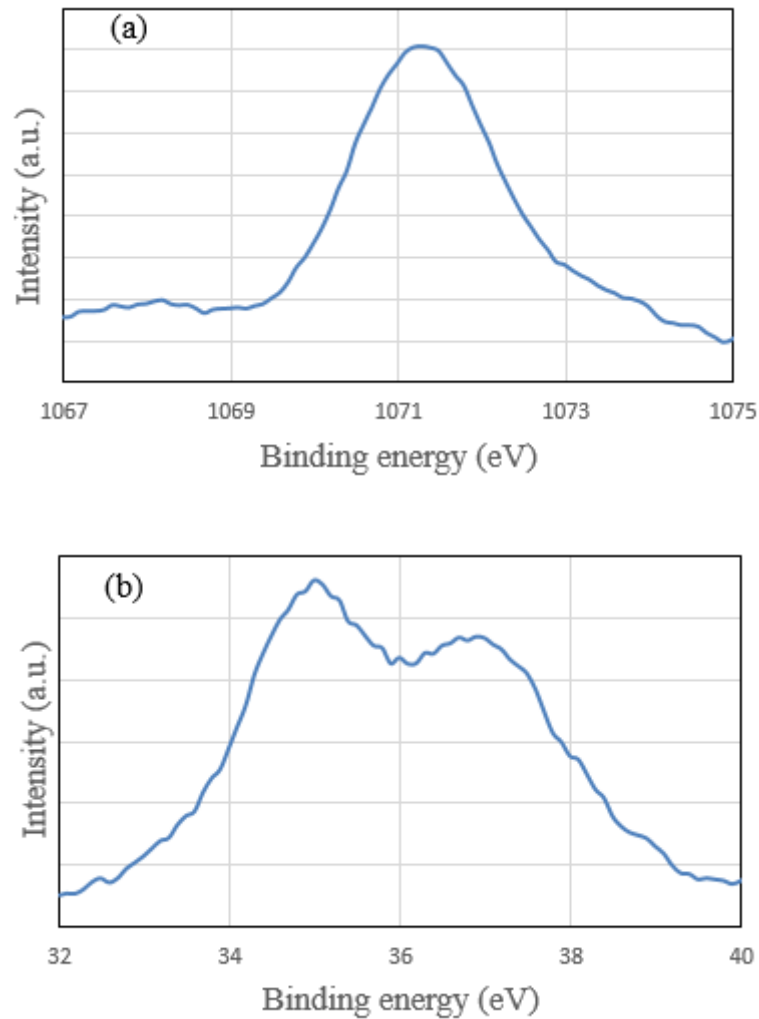


Fig. 5. XPS spectra of Na (a) and W (b) elements for the Na-W co-doped g-C₃N₄.

Using TEM analysis, the morphologies of the Na-W co-doped g-C₃N₄ specimen were studied. According to Fig. 6, the sample has a layered structure that is comparable to that of a graphite structure and is typical morphology for graphitic carbon nitride. These findings suggest that the collapse of the g-C₃N₄ skeleton is not triggered by the addition of Na and W

elements and that the skeleton retains its planar form. Some nanopores were observed in the samples. The creation of nanopores may be due to the release of CO₂ and NH₃ gases during the polymerization of the urea [30, 31]. These holes may be appropriate for reactive active sites and boosting catalytic activity.

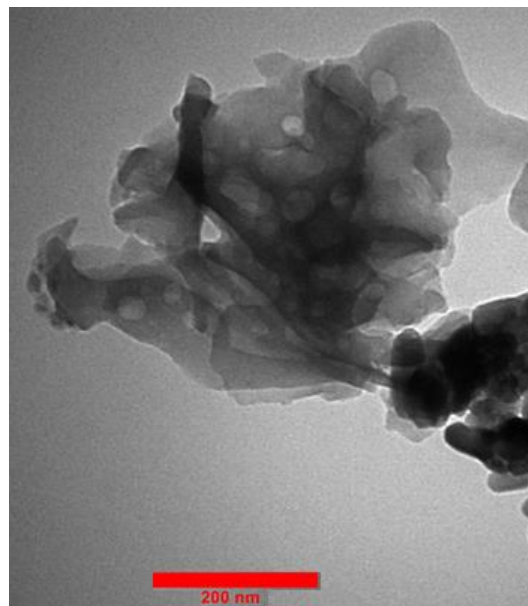


Fig. 6. TEM image of the Na-W co-doped g-C₃N₄.

The photocatalytic activities of bulk g-C₃N₄, exfoliated g-C₃N₄ and Na-W co-doped exfoliated g-C₃N₄ in the degradation of methylene blue under light irradiation are shown in Fig. 7. The reaction tube was constantly agitated in the dark for 30 minutes before to the start of the irradiation in order to establish the adsorption-desorption equilibrium. It is clear that tungsten and sodium ions doping increases the dye absorption of the graphitic carbon nitride in dark media, which is very important for better photocatalytic properties. As it is known, before the photodegradation, the pollutant should be attached to the active sites of the photocatalyst. Results from the control experiment show that methylene blue degrades via a photocatalytic process because the degradation process did not happen in the absence of either irradiation or a photocatalyst. Over bulk g-C₃N₄, less than 5% of methylene blue is destroyed in 90 minutes. The methylene blue photodegradation over exfoliated g-C₃N₄ is higher. The better photocatalytic property of the exfoliated sample is due to higher active sites, which is due to the delamination of layers of carbon nitride and its

surface oxidation. The dye removal activity of the Na-W co-doped exfoliated g-C₃N₄ sample is noticeably higher than those of pure bulk g-C₃N₄ and pure exfoliated g-C₃N₄. Based on the aforementioned findings, a potential mechanism for the W and Na co-doped photocatalyst could be proposed. First, electrostatic attraction caused the methylene blue to be absorbed on the surface of samples when it was mixed with the methylene blue solution. When the samples are exposed to light, electron-hole pairs are created. These photogenerated electrons and holes could react with water and adsorbed oxygen molecules to form radicals. These formed radicals may attack the organic dyes and degrade them. The better photocatalytic activity of Na-W co-doped samples may be because doping can facilitate the separation of the photogenerated electrons and holes in addition to decreasing the band gap.

The reaction rate constant (k) was calculated by equation 1 [32], as shown in Fig. 8.

$$-\ln\left(\frac{C}{C_0}\right) = kt \quad (\text{Eq. 1})$$

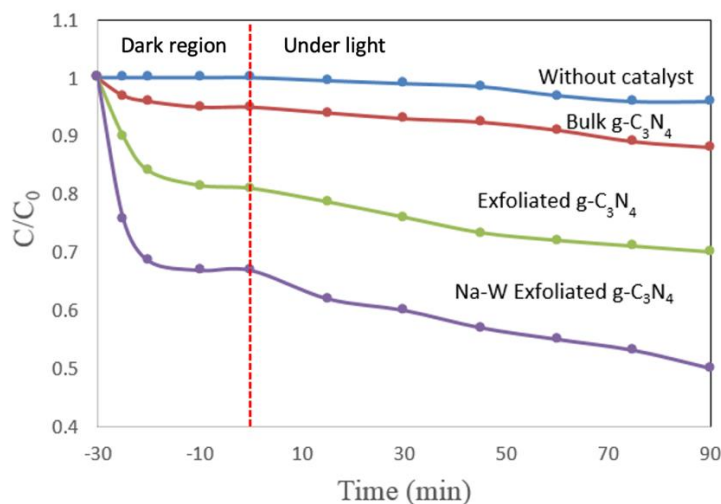


Fig. 7. Photodegradation of methylene blue over the samples.

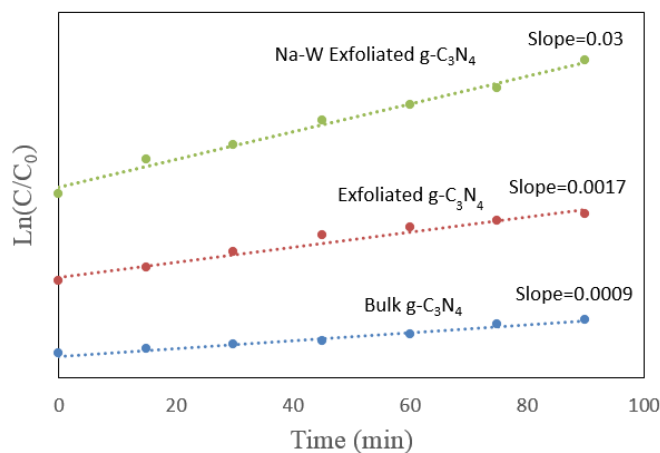


Fig. 8. Calculation of the reaction rate constant of samples for photodegradation of methylene blue.

where C and C_0 denote the amounts of pollutants at time t and t_0 , respectively. The irradiation time (t) versus $-\ln(C/C_0)$ plot is almost straight, and all samples have good correlation coefficients. According to the first-order model, the rate constant (k) of Na-W co-doped exfoliated $g-C_3N_4$ is 3.3 and 1.7 times higher than that of the pure bulk $g-C_3N_4$ and pure exfoliated $g-C_3N_4$, respectively. As it is known, the link between the amounts of reactants and the rate of a chemical reaction is shown by the k . A higher value for the k means a higher rate of reactions [33, 34]. Therefore, these results confirm that the doped samples have a higher potential for photocatalytic reactions.

4. Conclusion

In conclusion, we present an easy approach to bulk $g-C_3N_4$ modification with improved photocatalytic activity. By using an exfoliation, a sodium-tungsten co-doped $g-C_3N_4$ photocatalyst was produced. The XRD results showed the formation of crystalline carbon nitride. The doping process reduced the

crystallinity of the products. The samples had a layered morphology. The band gap energy of samples decreased by the addition of W and Na elements. The XPS analysis confirmed the existence of doping elements on the surface of samples. The photocatalytic activity for the photodegradation of methylene blue was improved compared with undoped samples.

References

- [1] S.R. Yousefi, H.A. Alshamsi, O. Amiri, M. Salavati-Niasari, "Synthesis, characterization and application of Co/Co₃O₄ nanocomposites as an effective photocatalyst for discoloration of organic dye contaminants in wastewater and antibacterial properties", *J. Mol. Liq.*, Vol. 337, 2021, pp. 116405.
- [2] X. Liu, R. Ma, L. Zhuang, B. Hu, J. Chen, X. Liu, X. Wang, "Recent developments of doped $g-C_3N_4$ photocatalysts for the degradation of organic pollutants", *Crit. Rev. Environ. Sci. Technol.*, Vol. 51, 2021, pp. 751–790.
- [3] J. Fu, J. Yu, C. Jiang, B. Cheng, " $g-C_3N_4$ -Based

- heterostructured photocatalysts", *Adv. Energy Mater.* Vol 8, 2018, pp. 1701503.
- [4] J. Wen, J. Xie, X. Chen, X. Li, "A review on g-C₃N₄-based photocatalysts", *Appl. Surf. Sci.*, Vol. 391, 2017, pp. 72–123.
- [5] S.A. Hassanzadeh-Tabrizi, C.C. Nguyen, T.O. Do, "Synthesis of Fe₂O₃/Pt/Au nanocomposite immobilized on g-C₃N₄ for localized plasmon photocatalytic hydrogen evolution", *Appl. Surf. Sci.*, Vol 489, 2019, pp. 741–754.
- [6] Y. Sheng, Z. Wei, H. Miao, W. Yao, H. Li, Y. Zhu, "Enhanced organic pollutant photodegradation via adsorption/photocatalysis synergy using a 3D g-C₃N₄/TiO₂ free-separation photocatalyst", *Chem. Eng. J.*, Vol. 370, 2019, pp. 287–294.
- [7] S. Ghattavi, A. Nezamzadeh-Ejhi, "A visible light driven AgBr/g-C₃N₄ photocatalyst composite in methyl orange photodegradation: focus on photoluminescence, mole ratio, synthesis method of g-C₃N₄ and scavengers", *Compos. Part. B. Eng.*, Vol. 183, 2020, pp. 107712.
- [8] M. Wu, H. Lv, T. Wang, Z. Ao, H. Sun, C. Wang, T. An, S. Wang, "Ag₂MoO₄ nanoparticles encapsulated in g-C₃N₄ for sunlight photodegradation of pollutants", *Catal. Today.*, Vol. 315, 2018, pp. 205–212.
- [9] H. Méndez, G. Heimel, A. Opitz, K. Suer, P. Barkowski, M. Oehzelt, J. Soeda, T. Okamoto, J. Takeya, J.B. Arlin, J.Y. Balandier, Y. Geerts, N. Koch, I. Salzmann, "Doping of organic semiconductors: impact of dopant strength and electronic coupling", *Angew. Chemie.*, Vol. 125, 2013, pp. 7905–7909.
- [10] S. Bera, D.I. Won, S.B. Rawal, H.J. Kang, W.I. Lee, "Design of visible-light photocatalysts by coupling of inorganic semiconductors", *Catal. Today.*, Vol. 335, 2019, pp. 3–19.
- [11] A.G. Akerdi, S.H. Bahrami, "Application of heterogeneous nano-semiconductors for photocatalytic advanced oxidation of organic compounds: a review", *J. Environ. Chem. Eng.*, Vol. 7, 2019, pp. 103283.
- [12] J. Wang, G. Wang, B. Cheng, J. Yu, J. Fan, "Sulfur-doped g-C₃N₄/TiO₂ Z-scheme heterojunction photocatalyst for Congo Red photodegradation", *Chinese J. Catal.*, Vol. 42, 2021, pp. 56–68.
- [13] G. Liu, M. Liao, Z. Zhang, H. Wang, D. Chen, Y. Feng, "Enhanced photodegradation performance of Rhodamine B with g-C₃N₄ modified by carbon nanotubes", *Sep. Purif. Technol.*, Vol. 244, 2020, pp. 116618.
- [14] M.M. Fang, J.X. Shao, X.G. Huang, J.Y. Wang, W. Chen, "Direct Z-scheme CdFe₂O₄/g-C₃N₄ hybrid photocatalysts for highly efficient cefotiofur sodium photodegradation", *J. Mater. Sci. Technol.*, Vol. 56, 2020, pp. 133–142.
- [15] D.S. Pattanayak, D. Pal, J. Mishra, C. Thakur, K.L. Wasewar, "Doped graphitic carbon nitride (g-C₃N₄) catalysts for efficient photodegradation of tetracycline antibiotics in aquatic environments", *Environ. Sci. Pollut. Res.*, Vol. 64, 2022, pp. 1–8.
- [16] A. Allahresani, B. Taheri, M.A. Nasser, "Fe (III)@ g-C₃N₄ nanocomposite-catalyzed green synthesis of di-indolyloxindole derivatives", *Res. Chem. Intermed.*, Vol. 44, 2018, pp. 6741–6751.
- [17] J. Ma, Q. Yang, Y. Wen, W. Liu, "Fe-g-C₃N₄/graphitized mesoporous carbon composite as an effective Fenton-like catalyst in a wide pH range", *Appl. Catal. B. Environ.*, Vol 201, 2017, pp. 232–240.
- [18] J. Tian, Q. Liu, C. Ge, Z. Xing, A.M. Asiri, A.O. Al-Youbi, X. Sun, "Ultrathin graphitic carbon nitride nanosheets: a novel peroxidase mimetic, Fe doping-mediated catalytic performance enhancement and application to rapid, highly sensitive optical detection of glucose", *Nanoscale*, Vol. 5, 2013, pp. 11604–11609.
- [19] L. Bi, D. Xu, L. Zhang, Y. Lin, D. Wang, T. Xie, "Metal Ni-loaded g-C₃N₄ for enhanced photocatalytic H₂ evolution activity: the change in surface band bending", *Phys. Chem. Chem. Phys.*, Vol. 17, 2015, pp. 29899–29905.
- [20] J. Zhang, S. Hu, Y. Wang, "A convenient method to prepare a novel alkali metal sodium doped carbon nitride photocatalyst with a tunable band structure", *RSC Adv.*, Vol. 4, 2014, pp. 62912–62919.
- [21] B. Liu, X. Nie, Y. Tang, S. Yang, L. Bian, F. Dong, H. He, Y. Zhou, K. Liu, "Objective findings on the K-doped g-C₃N₄ Photocatalysts: The presence and influence of organic byproducts on K-doped g-C₃N₄ photocatalysis", *Langmuir*, Vol. 37, 2021, pp. 4859–4868.
- [22] J. Zhao, L. Ma, H. Wang, Y. Zhao, J. Zhang, S. Hu, "Novel band gap-tunable K–Na co-doped graphitic carbon nitride prepared by molten salt method", *Appl. Surf. Sci.*, Vol. 332, 2015, pp. 625–630.
- [23] H. Wang, W. He, H. Wang, F. Dong, "In situ FT-IR investigation on the reaction mechanism of visible light photocatalytic NO oxidation with defective g-C₃N₄", *Sci. Bull.*, Vol. 63, 2018, pp. 117–125.
- [24] H. Yan, H. Yang, "TiO₂-g-C₃N₄ composite materials for photocatalytic H₂ evolution under visible light irradiation", *J. Alloys. Compd.*, Vol. 509, 2011, pp. 26–29.
- [25] R. Pournajaf, S.A. Hassanzadeh-Tabrizi, "Polyacrylamide synthesis of nanostructured copper aluminate for photocatalytic application", *J. Adv. Mater. Process.*, Vol. 5, 2018, pp. 12–19.
- [26] K. Wang, Q. Li, B. Liu, B. Cheng, W. Ho, J. Yu, "Sulfur-doped g-C₃N₄ with enhanced photocatalytic CO₂-reduction performance", *Appl. Catal. B. Environ.*, Vol. 176, 2015, pp. 44–52.

- [27] Z. Huang, Q. Sun, K. Lv, Z. Zhang, M. Li, B. Li, "Effect of contact interface between TiO_2 and g- C_3N_4 on the photoreactivity of g- $\text{C}_3\text{N}_4/\text{TiO}_2$ photocatalyst: (0 0 1) vs (1 0 1) facets of TiO_2 ", *Appl. Catal. B. Environ.*, Vol. 164, 2015, pp. 420–427.
- [28] S. Park, C.H. Champness, I. Shih, "Characteristics of XPS Se 3d peaks in crystalline Bridgman CuInSe_{2+x} with added sodium in the melt", *J. Electron. Spectros. Relat. Phenomena.*, Vol. 205, 2015, pp. 23–28.
- [29] L.L. Lai, J.M. Wu, "A facile solution approach to W, N co-doped TiO_2 nanobelt thin films with high photocatalytic activity", *J. Mater. Chem. A.*, Vol. 3, 2015, pp. 15863–15868.
- [30] Z.A. Lan, G. Zhang, X. Wang, "A facile synthesis of Br-modified g- C_3N_4 semiconductors for photoredox water splitting", *Appl. Catal. B. Environ.*, Vol. 192, 2016, pp. 116–125.
- [31] F. Guo, L. Wang, H. Sun, M. Li, W. Shi, X. Lin, "A one-pot sealed ammonia self-etching strategy to synthesis of N-defective g- C_3N_4 for enhanced visible-light photocatalytic hydrogen", *Int. J. Hydrogen. Energy.*, Vol. 45, 2020, pp. 30521–30532.
- [32] N. Al-Zaqri, A. Muthuvel, M. Jothibas, A. Alsalmeh, F.A. Alharthi, V. Mohana, "Biosynthesis of zirconium oxide nanoparticles using *Wrightia tinctoria* leaf extract: Characterization, photocatalytic degradation and antibacterial activities", *Inorg. Chem. Commun.*, Vol. 127, 2021, pp. 108507.
- [33] H.C. Yatmaz, A. Akyol, M. Bayramoglu, "Kinetics of the photocatalytic decolorization of an azo reactive dye in aqueous ZnO suspensions", *Ind. Eng. Chem. Res.*, Vol. 43, 2004, pp. 6035–6039.
- [34] Y. Li, X. Li, J. Li, J. Yin, "Photocatalytic degradation of methyl orange by TiO_2 -coated activated carbon and kinetic study", *Water. Res.*, Vol. 40, 2006, pp. 1119–1126.